Acta Astronautica 190 (2022) 342–348

Contents lists available at ScienceDirect

Acta Astronautica

journal homepage: www.elsevier.com/locate/actaastro

A theoretical criterion on the initiation type of oblique detonation waves

Xinxing Shi [a], Haopin Xie [a], Lin Zhou [a,b], Yining Zhang [a,*]

[a] Science and Technology on Scramjet Laboratory, Beijing Power Machinery Institute, Beijing, 100074, China
[b] School of Aerospace Engineering, Beijing Institute of Technology, Beijing, 100081, China

ARTICLE INFO

Keywords:
Detonation
Shock
Initiation type
Hydrogen

ABSTRACT

Predicting the initiation type of oblique detonation waves (ODWs) is critical to the application of ODWs in engine, but there is still no fully analytical criterion on the initiation type. In this study, a theoretical criterion is proposed to predict the initiation type, whose physical foundation is compression wave convergence observed recently. The criterion depends on the ratio of two characteristic lengths, the height of compression wave intersection point, H_{CW}, and the corresponding height of oblique shock wave (OSW) at the same x-location, H_{OSW}. If the ratio is below 1, the compression wave converges quickly to induce abrupt initiation; otherwise, slow compression wave convergence leads to smooth initiation. Because these two parameters could be calculated theoretically, this is the first fully analytical criterion independent of numerical or experimental parameters. Numerical results demonstrate that the criterion performs well in hydrogen–air mixtures corresponding wide flight conditions. Further examinations in two kinds of hydrocarbon fuel-based mixtures under standard conditions demonstrates the universality of this criterion.

1. Introduction

Detonation propulsion has attracted increasing attention in recent years [1–4]. A detonation wave usually consists of a strong leading shock with the subsequent heat release occurring at high pressure, which helps improve the thermal cycle efficiency of detonation engines. There are three types of detonation engines, named as PDE (Pulsating Detonation Engine), RDE (Rotating Detonation Engine), and ODE (Oblique Detonation Engine). Different from the complex detonation onset problem (usually the unsteady deflagration-to-detonation transition (DDT) process) in PDE and RDE [5–7], ODE achieves direct initiation of detonation by oblique shock waves (OSWs) generated by a wedge in supersonic combustible mixtures. The ODE is applicable to air-breathing hypersonic aircraft with higher flight Mach numbers than a conventional supersonic combustion ramjet (scramjet). Such hypersonic airbreathing propulsion devices are at the frontier of research in astronautics and aeronautics [8,9].

An ODE uses an oblique detonation wave (ODW) to release heat quickly in the combustion chamber, so the basic structure of the ODW should be investigated first. Pioneering numerical [10] and later experimental studies [11] revealed that the ODW structure consists of a non-reactive OSW, a set of deflagration waves, and the ODW surface, all united on a multi-wave point. However, subsequent study [12] demonstrated that the steady OSW-ODW transition structure also can consist of a curved shock front. The transition from the OSW to ODW could be viewed as ODW initiation. Generally, there exist two initiation types (steady OSW-ODW transition structures), abrupt and smooth. The former featured by a multi-wave point, while the latter featured by the curved shock. Several engineering-oriented studies [13–18] revealed that ODWs with different initiation types have different stability and thermodynamic efficiency characteristics, both of which are main concerns in practical application of ODWs. Therefore, some criteria for the initiation type prediction have been proposed, such as the angle difference [19] and the pressure ratio [20] between ODW and OSW. However, these criteria are usually limited to a narrow parametric range, which makes them hard to be generalized and used in engineering design of ODE.

To develop a universal criterion for initiation type, several studies have been conducted to clarify the features of ODW initiation region. Numerical investigations on structural variations have demonstrated that the initiation is usually abrupt at low inflow Mach number, high chemical activation energy, and small wedge angle [21–23]. Besides, ODW initiation in various fuel-based mixtures such as

Abbreviations: ODW, Oblique detonation wave; OSW, Oblique shock wave; ODE, Oblique detonation engine; CW, Compression wave; NDW, Normal detonation wave; DDT, Deflagration-to-detonation transition.

* Corresponding author.
E-mail address: 13718931527@163.com (Y. Zhang).

https://doi.org/10.1016/j.actaastro.2021.10.005
Received 20 August 2021; Received in revised form 26 September 2021; Accepted 4 October 2021
Available online 6 October 2021

Nomenclature

H_0	flight altitude
Ma_0	flight Mach number
M_0	inflow Mach number
P	pressure
T	temperature
V	velocity
ρ	density
H_{CW}	height of compression wave intersection point
H_{OSW}	corresponding height of oblique shock wave at the same x-location
α	Mach line angle
β	oblique shock angle
θ	wedge angle
φ	flow deflection angle
$\tilde{\dot{\sigma}}$	normalized heat release rate
w_i	molecular weight
$\overline{w}$	mean molecular weight
ω_i	mass production rate
h_i	specific enthalpy
γ	specific heat ratio
n	species' number
c_p	frozen specific heat
Y_i	species' mass fraction

acetylene–oxygen–argon were also investigated recently, revealing new wave structures in initiation region [24–26]. Although extensive studies have been conducted on the initiation characteristics, there was still no single underlying physical model for the ODW classical structure triggered by a semi-infinite wedge, due to the complicated nonlinear coupling of shock and chemical reaction under high-speed inflow. As a matter of fact, even for the classical two-dimensional normal detonation wave, we still only have relatively few semi-theoretical approaches to predict the cell size [27–29]. A recent study [30] proposed a semi-theoretical criterion from the perspective of compression wave (CW) convergence to analyze wave system evolution in ODW initiation region, which shined some new light on ODW initiation type prediction. However, the criterion has to rely on parameters coming from numerical simulation, so we still lack a fully analytical criterion to predict the initiation type.

In this study, a fully analytical criterion independent of numerical or experimental parameters is proposed to predict the initiation type of ODWs for the first time. The criterion depends on the ratio of two theoretically characteristic lengths, which can quantify the wave system interaction of the initiation region. The newly proposed criterion is applied to three kinds of combustible mixtures with different inflow conditions, demonstrating its universality for predicting the initiation type of ODWs.

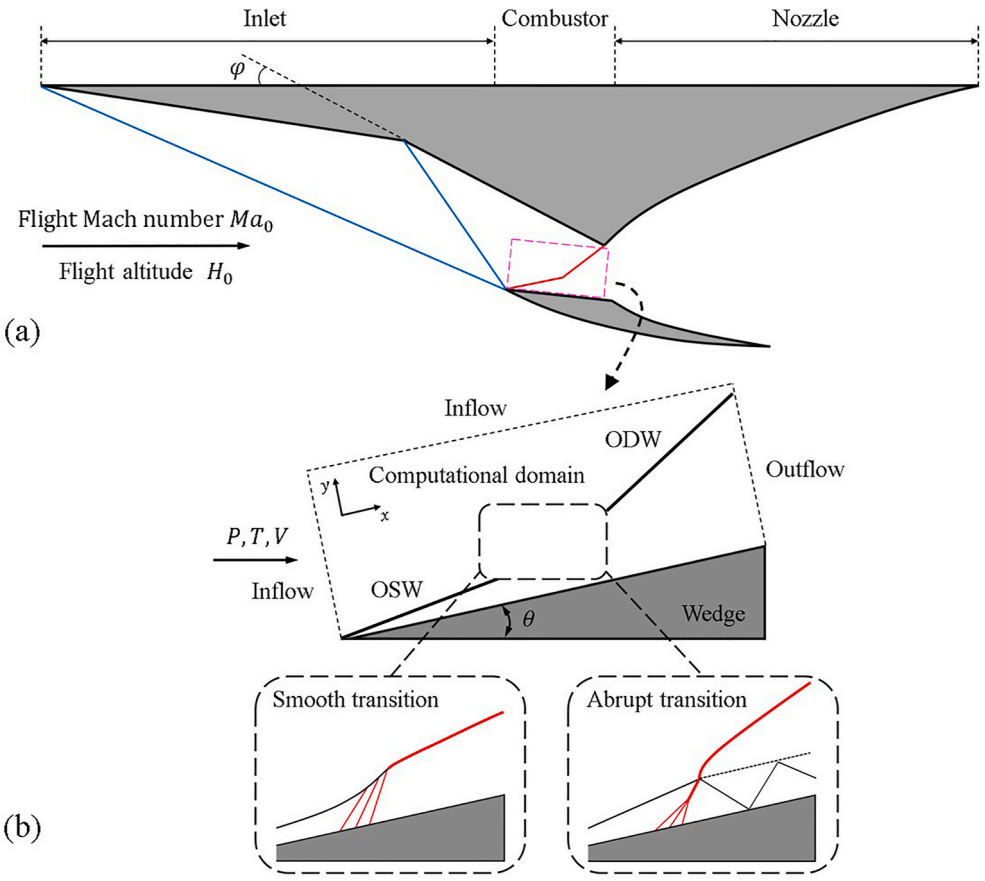

Fig. 1. Schematic of an ODE (a) and the wedge-induced ODW computation domain (b).

2. Model and method

2.1. Simulation model and computational method

Fig. 1 shows the schematic of an ODE and the computational settings of a wedge-induced ODW. The ODE inlet configuration follows many previous studies [31,32], in which two equal-strength shocks were used to slow and pressurize hypersonic air inflow at high flight altitude. Then, the fuel and air are assumed to be well premixed in the inlet, and the total pressure loss caused by the fuel injection is neglected. The supersonic combustible mixture reflects on the two-dimensional wedge and first generates an OSW, which triggers exothermic chemical reactions owing to the high post-shock temperature and subsequently induces ODW initiation downstream. In this study, the computational domain is enclosed by the dashed line in Fig. 1(b), in which two typical initiation types, smooth and abrupt initiation, are illustrated. Rotating the coordinates to the direction along the wedge surface aligns the Cartesian grid in the rectangular domain with the wedge surface.

The simulation and analysis are based on the reactive Euler equations following previous numerical works [33–37]. The numerical code has been used and tested for many other studies focusing on different aspects of ODW characteristic [14,23,26,30], ensuring the results obtained in this study to be trustworthy. The chemical kinetic model in this study is taken from a comprehensive H_2/O_2 kinetic mechanism suitable for high-pressure combustion [38] that involves 27 reversible elementary reactions among 8 species (H_2, O_2, H_2O, H, O, OH, HO_2, and H_2O_2) with 5 inert species (N_2, Ar, He, CO, and CO_2). The thermodynamic properties of the chemical species are evaluated using the nine-coefficient NASA polynomial representation [39]. The governing equations are discretized on Cartesian uniform grids and solved using the dispersion-controlled dissipation (DCD) scheme [40] with Strang splitting. To overcome the stiffness problem in solving the detailed chemical reaction process, a sufficient number of sub-reaction steps are involved to ensure overall accuracy of simulation results [41]. Moreover, some studies [42,43] show that the accumulation of errors is not negligible for large scale simulations of complex unsteady combustion gas dynamics such as DDT otherwise, leading to unreliable detonation initiation. However, this work focuses on the steady OSW-ODW transition structures in steady flow field rather than unsteady process of the detonation initiation, which are insensitive to unsteady state flows and error accumulation with time. Therefore, the present work does not involve the problem of accumulation of errors.

Both the left and upper boundaries of the computational domain have inflow conditions fixed at the free-stream values. The outflow conditions used on the right and lower boundaries before the wedge are extrapolated from the interior assuming zero first-order derivatives. A slip boundary condition is implemented on the wedge surface, which starts from $x = 0$ mm on the lower computational boundary. Initially, the whole flow field has uniform density, velocity, and pressure, all of which are calculated according to the inflow conditions and the wedge angle θ. In all subsequent figures, the dimensions of temperature, pressure, density, and heat release rate are K, Pa, kg/m^3, and kJ/(cm^3.s), respectively.

2.2. Theoretical method

In this study, both the flight altitude H_0 and Mach number Ma_0 are chosen as the controlling parameters to avoid artificial parametric settings and to cover a wide range of flight conditions. For different simulation cases, the default wedge angle is 19°, and both flow deflection angles are varied to keep the total deflection angle of ODE inlet compression fixed at 24°. The default inflow is set to be a homogeneous stoichiometric hydrogen–air mixture with H_2:O_2:N_2 = 2:1:3.76 in all cases. The detailed method of calculating pre-detonation parameters for each case can be found in Refs. [14,44].

Two cases corresponding to $H_0 = 30$ km are first simulated with the flight Mach number Ma_0 equal to 9.5 and 8.5. The temperature fields and pressure contours are shown in Fig. 2, from which two typical ODW initiation structures can be observed. Both structures consist of an OSW and an ODW, which are connected by a curve shock at $Ma_0 = 9.5$ (Fig. 2 (a)) but connected by a multi-wave point at $Ma_0 = 8.5$ (Fig. 2(b)). The former corresponds to smooth initiation and the latter to abrupt initiation. One of the main distinctions between the two initiation types is the wave system of the initiation region, in which the heat release induces the CW. This is indicated by the pressure contours in front of the main heat release layer. The CW generated by the heat addition of the supersonic flow converges gradually, but its degree of convergence varies in different cases. The CW and its convergence are modest, and it finally converges above the OSW at $Ma_0 = 9.5$. Thus, the CW gradually interacts with the main OSW, which deflects gradually and transitions to the ODW. In contrast, the CW converges quickly and becomes strong at $Ma_0 = 8.5$, resulting in the oblique shock. Coupled with the reactive front, the oblique shock generated by CW convergence leads to a secondary ODW with short length that interacts intensely with the main OSW and induces abrupt initiation. Aforementioned analysis demonstrates that the degree of CW convergence is critical to determine the initiation type variation of ODWs.

According to the previous study [30], the CW convergence can be described by the variations of parameters along the streamline of wedge surface. The temperature variation along the streamline of $y = 0$ m for $Ma_0 = 8.5$ and $H_0 = 30$ km is shown in Fig. 3(a). After the combustible mixture is compressed by the OSW, the temperature of shocked flow increases gradually due to the heat release of chemical reaction. The heat addition in the supersonic flow generates the CW and results in the decrease of local Mach number. Therefore, the angles of the Mach lines derived from the streamline of $y = 0$ m increase gradually from upstream to downstream as shown in Fig. 3(a). Similar processes occur along other x axis parallel streamlines, so the CW will converge finally. Despite of a stationary flow field, this compression wave distribution can be viewed as a convergence from the bottom-up, named as 'CW convergence'. It is necessary to note that 'the initiation types' investigated in this paper refers to the steady OSW-ODW transition structures, rather not the detailed transient initiation process of ODW. In addition, it is worth noting that the initiation of ODWs is instantaneous without going through the pre-detonation stage of flame acceleration of DDT [45–47], which corresponds to the other scenario of detonation onset with extensively studies. The wave system interaction between OSW and CW with different convergence degree in the initiation region leads to the initiation type variation of ODWs.

To quantify the wave system interaction of the initiation region and finally predict the initiation type, a fully analytical criterion was proposed based on the ratio of two theoretically characteristic lengths, H_{CW} and H_{OSW}. The former is the height of the CW, H_{CW}, defined by the height of the intersection of two characteristic Mach lines, was used to quantify the CW convergence. The latter is the theoretical height of the OSW, defined by the y-height of the OSW at the same x-location as that of the CW intersection point. If the ratio is below 1, the CW converges quickly to induce abrupt initiation; otherwise, the slow heat release leads to smooth initiation. Since both H_{CW} and H_{OSW} can be calculated through completely theoretical calculation, the newly proposed criterion provides fully analytical tool for initiation type prediction of ODWs independent of numerical or experimental parameters.

Because the theoretical calculation method of OSW is simple, the y-height of the OSW can be calculated immediately as soon as the CW intersection point is obtained. Hence, the key to this theoretical criterion is to determine H_{CW}, which can be done using two characteristic Mach lines as illustrated in Fig. 3(b). The CW front is denoted by the first orange Mach line, starting from the x-axis at the point where the heat release rate reaches 10% of its peak value along the near-wedge streamline. The CW tail is denoted by the second red Mach line, starting from the x-axis at the point where the maximum heat release rate is achieved. It should be noted that, for the flow considering viscosity, the

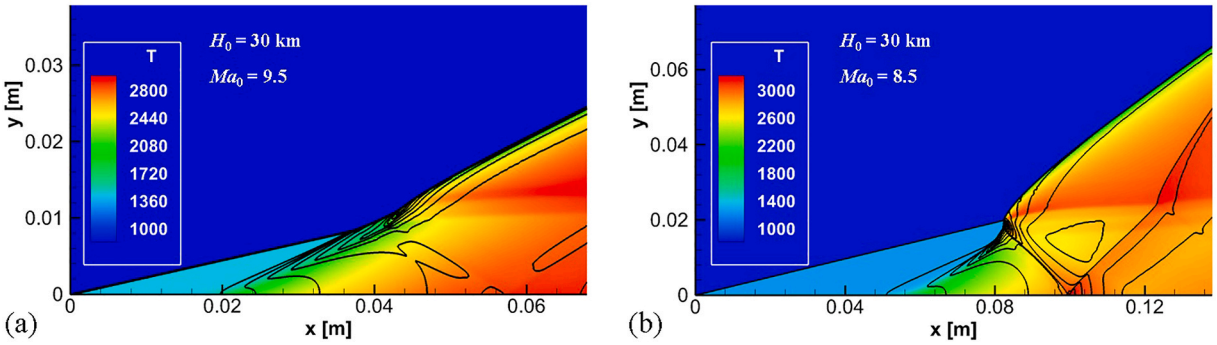

Fig. 2. Temperature fields and pressure contours with $H_0 = 30$ km for $Ma_0 = 9.5$ and 8.5.

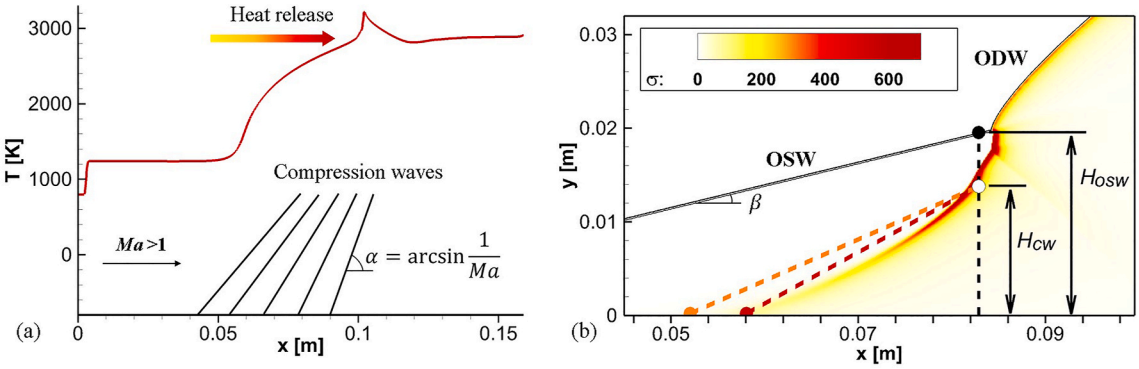

Fig. 3. (a) Temperature along the streamline of $y = 0$ m for $Ma_0 = 8.5$ and $H_0 = 30$ km and schematic of Mach lines of supersonic flow with heat addition. (b) Enlarged initiation zone of heat release field for $Ma_0 = 8.5$ and $H_0 = 30$ km. (The orange and red dashed lines are the characteristic Mach lines of the induction zone and heat release zone along $y = 0$ m, respectively.). (For interpretation of the references to colour in this figure legend, the reader is referred to the Web version of this article.)

CW appears due to boundary layer growth and ignition of mixture along the wedge surface. In addition, the flow of the near-wedge streamline is essentially subsonic, thus Mach lines do not exist because the equations are not hyperbolic. However, for the inviscid flow field studied in this paper, we mainly focus on the CW induced by the chemical reaction in supersonic flow. Under the inviscid assumption, the inclination angle of the Mach line is calculated from the local flow Mach number according to Eq. (1), resulting in an intersection point at a distance from the wedge of H_{CW}:

$$\sin\alpha = \frac{1}{Ma}. \tag{1}$$

The detailed interaction of flow and heat release along the near-wedge streamline can be easily estimated using the methods of calculating Zel'dovich–von Neumann–Döring (ZND) structures of one-dimensional steady detonations; thus, H_{CW} can be determined theoretically. Given the mixture inflow parameters P, T, V, and the wedge angle θ, we can calculate the gas parameters after compression by the main OSW using the Rankine–Hugoniot relations for the given OSW angle β. Then, the following equations [48] are integrated from the post-shock state and the beginning of the wedge surface:

$$\frac{d\rho}{dx} = -\frac{\rho\dot{\tilde{\sigma}}}{V(1-Ma^2)}, \tag{2}$$

$$\frac{dV}{dx} = \frac{\dot{\tilde{\sigma}}}{1-Ma^2}, \tag{3}$$

$$\frac{dP}{dx} = -\frac{\rho V\dot{\tilde{\sigma}}}{1-Ma^2}, \tag{4}$$

$$\frac{dY_i}{dx} = -\frac{\omega_i}{\rho V}. \tag{5}$$

The normalized heat release rate $\dot{\tilde{\sigma}}$ is calculated via

$$\dot{\tilde{\sigma}} = \sum_{i=1}^{n}\left(\frac{\overline{w}}{w_i} - \frac{h_i}{c_pT}\right)\frac{dY_i}{dt}, \tag{6}$$

where $\overline{w}$ is the mean molecular weight of the mixture, c_p is the frozen specific heat of the mixture, and Y_i is the mass fraction of the species. Once the equations are solved, the heat release rate and Mach number along the wedge streamline can be obtained. Thereafter, the CW intersection point and corresponding theoretical H_{CW} can be calculated following the above procedure.

It is easy to calculate the OSW angle β by solving Eq. (7) when the wedge angle θ and inflow parameters are given. Thus, the theoretical H_{OSW} can be easily obtained according to the x-location of the CW intersection point and the OSW angle β:

$$\tan^3\beta + A\tan^2\beta + B\tan\beta + C = 0, \tag{7}$$

where

$$\left.\begin{aligned} A &= \frac{1-Ma^2}{\tan\theta[1+(\gamma-1)Ma^2/2]},\\ B &= \frac{1+(\gamma+1)Ma^2/2}{1+(\gamma-1)Ma^2/2},\\ C &= \frac{1}{\tan\theta[1+(\gamma-1)Ma^2/2]} \end{aligned}\right\} \tag{8}$$

3. Results and discussion

3.1. Hydrogen–air mixture corresponding wide flight conditions

To verify the prediction method proposed in Sec.2, we analyze more cases with a wide range of flight Mach numbers and altitudes in this section. Fig. 4 shows the simulated flow fields and prediction results for different Ma_0 values with a fixed H_0 = 30 km. We see that the ODW initiation type varies with Ma_0. The initiation is smooth for Ma_0 = 10, in which case the CW converges slowly. The two characteristic Mach lines intersect the OSW successively and finally converge to the CW intersection point (denoted by the white point), which is above the OSW (denoted by the black point), thus H_{CW}/H_{OSW} is above 1. As Ma_0 decreases from 10 to 9, the two characteristic Mach lines converge modestly and the convergence point happens to intersect with the OSW (H_{CW}/H_{OSW} nearly equals to 1), which causes an initiation that is intermediate between smooth and abrupt. Further decreasing Ma_0 to 8, however, causes the initiation type to change to obviously abrupt. Meanwhile, the CW intersection point is below the OSW with H_{CW}/H_{OSW} less than 1 because of the rapid CW convergence, leading to a long normal detonation wave (NDW) beneath the transition point. Thus, these cases demonstrate that the two characteristic lengths, H_{CW} and H_{OSW}, well quantify the CW convergence and its effect on ODW initiation structure, and hence well predict the initiation type.

Fig. 5 presents more cases with different Ma_0 and H_0 values with H_{OSW} and H_{CW} calculated using the proposed theoretical method. Abrupt and smooth initiations are represented by solid and hollow symbols, respectively. In the parametric ranges considered in this study, i.e., H_0 = 10–40 km and Ma_0 = 8–10, the initiation is smooth at high H_0 and Ma_0, and abrupt at low H_0 and Ma_0.

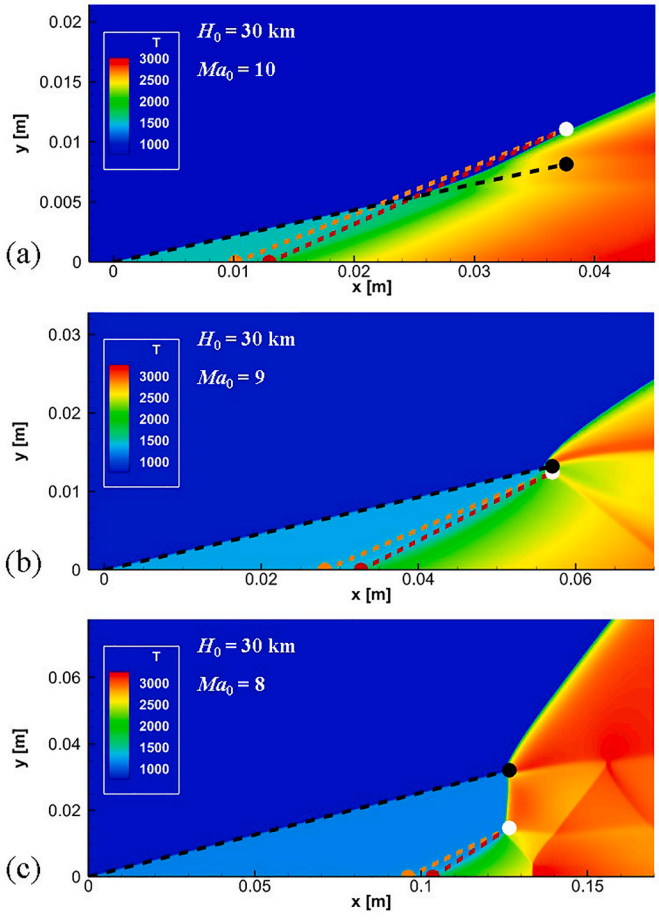

Fig. 4. Temperature fields with pressure contours and prediction results for H_0 = 30 km and Ma_0 = 10, 9, and 8.

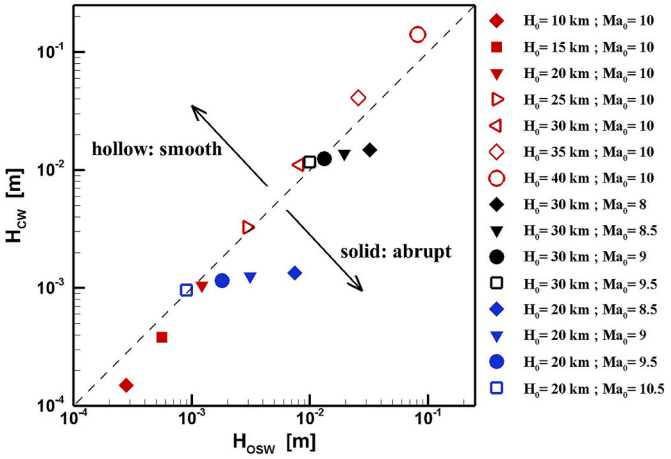

Fig. 5. Theoretical results for H_{OSW} and H_{CW} with corresponding initiation type in a stoichiometric hydrogen–air mixture at different flight Mach numbers and altitudes.

Obviously, H_{CW} increases when H_0 increases with Ma_0 fixed at 10; H_{OSW} follows the same trend as H_{CW} but increases more modestly. The initiation changes from abrupt to smooth as H_0 increases. When H_0 is constant and Ma_0 decreases, both H_{CW} and H_{OSW} increase but H_{OSW} changes more rapidly, and the initiation varies from smooth to abrupt. Overall, when the ratio of H_{CW} and H_{OSW} is below 1, CW convergence is fast and induces abrupt initiation; otherwise, CW convergence is slow and leads to smooth initiation. The two initiation types can be well distinguished by the dashed line where the ratio equals to 1 in Fig. 5. The solid symbols obtained through theoretical calculation below the line in Fig. 5 reflect abrupt initiation, while the hollow ones above it reflect smooth initiation. Therefore, the diagonal in the coordinate system composed of H_{CW} and H_{OSW} can be used as a criterion to predict the initiation type.

3.2. Extension to hydrocarbon fuel-based mixtures

Previous studies [24,25] have demonstrated that mixture properties significantly influence ODW structures; thus, further tests on ODWs in hydrocarbon fuel-based mixtures were performed to verify the universality of the criterion.

We first examined ODWs in a stoichiometric acetylene–oxygen–argon mixture diluted with 85% argon, so C_2H_2: O_2: AR = 2 : 5: 39.67. The chemical kinetic model used for this mixture was taken from an acetylene–oxygen–diluent chemical mechanism for high pressure [49]. The computational domain and simulation method were the same as in Sec. 2, except that the standard inflow parameters were used instead of the flight conditions before the wedge and the wedge angle was fixed at 25°. Fig. 6 shows the simulation and prediction results when the inflow Mach number M_0 varied from 7 to 10.

We observe that the ODW structures are significantly influenced by M_0, and the initiation type changes from smooth to abrupt when M_0 decreases from 10 to 7. Meanwhile, the degree of CW convergence is gradually enhanced according to the two characteristic Mach lines in the initiation region, which leads to the smooth initiation achieved by a curved shock at M_0 = 10 and 9, the intermediate initiation at M_0 = 8, and the abrupt initiation achieved by a multi-wave point at M_0 = 7. The variation in initiation structure with inflow Mach number is similar to that of the above hydrogen–air mixture, although the inflow conditions are different. The predicted CW intersection point (black point) changes from higher than the OSW at M_0 = 10 and 9 (white point) to lower than the OSW at M_0 = 8 and 7 (white point). Therefore, the theoretical predictions are consistent with the simulation results, indicating that the

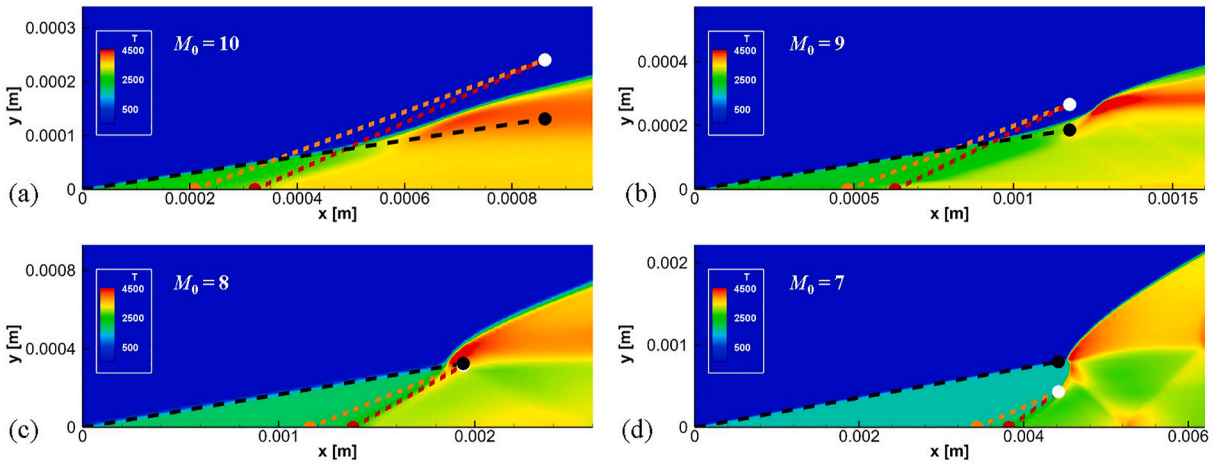

Fig. 6. Temperature fields with pressure contours and prediction results for a stoichiometric acetylene–oxygen mixture with 85% argon dilution in standard conditions for M_0 = 10, 9, 8, and 7.

theoretical criterion is also applicable to the ODWs in the acetylene–oxygen–argon mixture.

ODWs in a methane–air mixture were also examined in this study. The computational settings were the same as those of the acetylene-based mixtures except that a larger wedge angle, 30°, was used owing to the hard initiation of ODWs in methane–air mixtures. The detailed chemical kinetic model used for methane–air was taken from a reduced mechanism [50] based on GRI-3.0. In the simulation, a stoichiometric methane–air mixture with CH_4: O_2: N_2 = 1 : 2: 7.52 was used, and the inflow Mach number M_0 was varied from 9 to 12. Fig. 7 shows the simulated initiations and theoretical predictions for all cases. The results for the acetylene–oxygen–argon mixture are also presented in Fig. 7.

As seen from Fig. 7, the initiation types are influenced by inflow Mach number M_0 for both the acetylene-based and methane-based mixtures, which also have similar trends. The theoretical results for both H_{CW} and H_{OSW} increase as M_0 decreases, but the rapid change in H_{OSW} results in its increasing from less than H_{CW} to greater than H_{CW}. In the meantime, the ODW initiation type changes from smooth to abrupt, which is due to the gradually enhanced CW convergence. Overall, the CW converges quickly to induce abrupt initiation at low M_0, at which H_{CW}/H_{OSW} is below 1. In contrast, the slow CW convergence leads to smooth initiation at high M_0, at which H_{CW}/H_{OSW} is above 1. Therefore, it is consistent with Fig. 5 that the part of Fig. 7 above the dashed line corresponds to smooth initiation while the part below the line reflects abrupt initiation. In summary, the ratio of two theoretical characteristic lengths, H_{CW} and H_{OSW}, perform well in predicting the ODW initiation type in hydrocarbon fuel-based mixtures, which further demonstrates the universality of the proposed theoretical criterion.

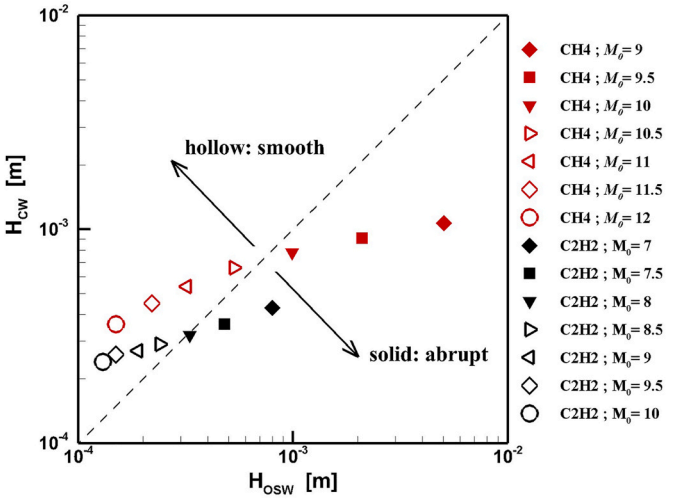

Fig. 7. Theoretical results for H_{OSW} and H_{CW} with corresponding initiation types in hydrocarbon fuel-based mixtures at different inflow Mach numbers.

4. Conclusion

The ODW initiation structure triggered by a semi-infinite wedge was studied numerically and theoretically to predict the initiation type of ODWs. The first fully analytical criterion was proposed based on the physical model of compression wave convergence from the perspective of wave system evolution in initiation region. This theoretical method depends on the ratio of two characteristic lengths, the height of compression wave intersection point, H_{CW}, and the corresponding height of OSW at the same x-location, H_{OSW}, both of which can be quickly calculated theoretically. Analytical results revealed that compression wave convergence is fast and induces abrupt initiation when the ratio is below 1, and heat release is slow and leads to smooth initiation when the ratio is above 1. The criterion can predict well the initiation type of ODWs in a hydrogen–air mixture in wide ranges of the ODE flight Mach number and altitude. Further simulations of ODWs in acetylene–oxygen–argon and methane–air mixtures with variable inflow Mach numbers in standard conditions demonstrated that the criterion is applicable to ODWs in hydrocarbon fuel-based mixtures. This fully theoretical criterion provides a universal and convenient tool to predict the initiation type of ODWs, which can help practical applications of ODEs.

Declaration of competing interest

The authors declare that they have no known competing financial interests or personal relationships that could have appeared to influence the work reported in this paper.

References

[1] P. Wolański, Detonative propulsion, Proc. Combust. Inst. 6 (2013) 125–158, https://doi.org/10.1016/j.proci.2012.10.005.
[2] M. Valorani, M.D. Giacinto, C. Buongiorno, Performance prediction for oblique detonation wave engines (ODWE), Acta Astronaut. 48 (2001) 211–228, https://doi.org/10.1016/S0094-5765(00)00161-2.
[3] B. Wang, J.P. Wang, Introduction to the special section on recent progress on rotating detonation and its application, AIAA J. 58 (2020) 4974–4975, https://doi.org/10.2514/1.J060144.

[4] S.J. Liu, H.Y. Peng, W.D. Liu, H.L. Zhang, Realization of methane-air continuous rotating detonation wave, Acta Astronaut. 164 (2019) 1–8, https://doi.org/10.1016/j.actaastro.2019.09.038.

[5] V.F. Nikitin, V.R. Dushin, Y.G. Phylippov, J.C. Legros, Pulse detonation engines: technical approaches, Acta Astronaut. 64 (2009) 281–287, https://doi.org/10.1016/j.actaastro.2008.08.002.

[6] N.N. Smirnov, V.F. Nikitin, L.I. Stamov, E. V Mikhalchenko, V.V. Tyurenkova, Three-dimensional modeling of rotating detonation in a ramjet engine, Acta Astronaut. 163 (2019) 168–176, https://doi.org/10.1016/j.actaastro.2019.02.016.

[7] N.N. Smirnov, V.B. Betelin, V.F. Nikitin, Y.G. Phylippov, J. Koo, Detonation engine fed by acetylene-oxygen mixture, Acta Astronaut. 104 (2014) 134–146, https://doi.org/10.1016/j.actaastro.2014.07.019.

[8] D.A. Rosato, M. Thornton, J. Sosa, C. Bachman, G.B. Goodwin, K.A. Ahmed, Stabilized detonation for hypersonic propulsion, Proc. Natl. Acad. Sci. Unit. States Am. 116 (2020), https://doi.org/10.1073/pnas.2102244118 e2102244118.

[9] Z. Jiang, Z. Zhang, Y. Liu, C. Wang, C. Luo, Criteria for hypersonic airbreathing propulsion and its experimental verification, Chin. J. Aeronaut. 34 (2021) 94–104, https://doi.org/10.1016/j.cja.2020.11.001.

[10] C. Li, K. Kailasanath, E.S. Oran, Detonation structures behind oblique shocks, Phys. Fluids 6 (1994) 1600–1611, https://doi.org/10.1063/1.868273.

[11] C. Viguier, L.F. Figueira Da Silva, D. Desbordes, B. Deshaies, Onset of oblique detonation waves: comparison between experimental and numerical results for hydrogen–air mixture, Symposium (International) on Combustion 26 (1996) 3023–3031, https://doi.org/10.1016/S0082-0784(96)80146-9.

[12] L.F. Figueira da Silva, B. Deshaies, Stabilization of an oblique detonation wave by a wedge: a parametric numerical study, Combust. Flame 121 (2000) 152–166, https://doi.org/10.1016/S0010-2180(99)00141-8.

[13] S. Miao, J. Zhou J, Z. Lin, X. Cai, S. Liu, Numerical study on thermodynamic efficiency and stability of oblique detonation waves, AIAA J. 56 (2018) 3112–3122, https://doi.org/10.2514/1.J056887.

[14] J. Bian, L. Zhou, H. Teng, Structural and thermal analysis on oblique detonation influenced by different forebody compressions in hydrogen–air mixtures, Fuel 286 (2021) 119458, https://doi.org/10.1016/j.fuel.2020.119458.

[15] T. Wang, Y. Zhang, H. Teng, Z. Jiang, H.D. Ng, Numerical study of oblique detonation wave initiation in a stoichiometric hydrogen–air mixture, Phys. Fluids 27 (2015) 96101, https://doi.org/10.1063/1.4930986.

[16] P. Yang, H.D. Ng, H. Teng, Numerical study of wedge–induced oblique detonations in unsteady flow, J. Fluid Mech. 876 (2019) 264–287, https://doi.org/10.1017/jfm.2019.542.

[17] K. Wang, Z. Zhang, P. Yang, H. Teng, Numerical study on reflection of an oblique detonation wave on an outward turning wall, Phys. Fluids 32 (2020) 46101., https://doi.org/10.1063/5.0001845.

[18] K. Wang, H. Teng, P. Yang, H.D. Ng, Numerical investigation of flow structures resulting from the interaction between an oblique detonation wave and an upper expansion corner, J. Fluid Mech. 903 (2020) A28, https://doi.org/10.1017/jfm.2020.644.

[19] H.H. Teng, Z.L. Jiang, On the transition pattern of the oblique detonation structure, J. Fluid Mech. 713 (2012) 659–669, https://doi.org/10.1017/jfm.2012.478.

[20] S. Miao, J. Zhou, S. Liu, X. Cai, Formation mechanisms and characteristics of transition patterns in oblique detonations, Acta Astronaut. 142 (2018) 121–129, https://doi.org/10.1016/j.actaastro.2017.10.035.

[21] P. Yang, H. Teng, Z. Jiang, H.D. Ng, Effects of inflow Mach number on oblique detonation initiation with a two–step induction–reaction kinetic model, Combust. Flame 193 (2018) 246–256, https://doi.org/10.1016/j.combustflame.2018.03.026.

[22] Y. Zhang, L. Zhou, J. Gong, H.D. Ng, H. Teng, Effects of activation energy on the instability of oblique detonation surfaces with a one–step chemistry model, Phys. Fluids 30 (2018) 106110, https://doi.org/10.1063/1.5054063.

[23] H. Teng, H.D. Ng, Z. Jiang, Initiation characteristics of wedge–induced oblique detonation waves in a stoichiometric hydrogen–air mixture, Proc. Combust. Inst. 36 (2017) 2735–2742, https://doi.org/10.1016/j.proci.2016.09.025.

[24] Y. Fang, Y. Zhang, X. Deng, H. Teng, Structure of wedge–induced oblique detonation in acetylene–oxygen–argon mixtures, Phys. Fluids 31 (2019) 26108, https://doi.org/10.1063/1.5086235.

[25] Y. Zhang, Y. Fang, H.D. Ng, H. Teng, Numerical investigation on the initiation of oblique detonation waves in stoichiometric acetylene–oxygen mixtures with high argon dilution, Combust. Flame 204 (2019) 391–396, https://doi.org/10.1016/j.combustflame.2019.03.033.

[26] C. Tian, H. Teng, H.D. Ng, Numerical investigation of oblique detonation structure in hydrogen–oxygen mixtures with Ar dilution, Fuel 252 (2019) 496–503, https://doi.org/10.1016/j.fuel.2019.04.126.

[27] A.I. Gavrikova, A.A. Efimenkoa, S.B. Dorofeeva, A model for detonation cell size prediction from chemical kinetics, Combust. Flame 120 (2000) 19–33, https://doi.org/10.1016/S0010-2180(99)00076-0.

[28] H.D. Ng, Y.J. John, H.S. Leeb, Assessment of detonation hazards in high–pressure hydrogen storage from chemical sensitivity analysis, Int. J. Hydrogen Energy 32 (2007) 93–99, https://doi.org/10.1016/j.ijhydene.2006.03.012.

[29] J.E. Shepherd, Detonation in gases, Proc. Combust. Inst. 32 (2009) 83–98, https://doi.org/10.1016/j.proci.2008.08.006.

[30] H. Teng, C. Tian, Y. Zhang, L. Zhou, H.D. Ng, Morphology of oblique detonation waves in a stoichiometric hydrogen–air mixture, J. Fluid Mech. 913 (2021) A1, https://doi.org/10.1017/jfm.2020.1131.

[31] R. Dudebout, J.P. Sislian, R. Oppitz, Numerical simulation of hypersonic shock–induced combustion ramjets, J. Propul. Power 14 (1998) 869–879, https://doi.org/10.2514/2.5368.

[32] J.P. Sislian, H. Schirmer, R. Dudebout, J. Schumacher, Propulsive performance of hypersonic oblique detonation wave and shock–induced combustion ramjets, J. Propul. Power 17 (2001) 599–604, https://doi.org/10.2514/2.5783.

[33] J. Verreault, A.J. Higgins, R.A. Stowe, Formation of transverse waves in oblique detonations, Proc. Combust. Inst. 34 (2013) 1913–1920, https://doi.org/10.1016/j.proci.2012.07.040.

[34] J.Y. Choi, E.J.R. Shin, I.S. Jeung, Unstable combustion induced by oblique shock waves at the non–attaching condition of the oblique detonation wave, Proc. Combust. Inst. 32 (2009) 2387–2396, https://doi.org/10.1016/j.proci.2008.06.212.

[35] H.H. Teng, Z.L. Jiang, H.D. Ng, Numerical study on unstable surfaces of oblique detonations, J. Fluid Mech. 744 (2014) 111–128, https://doi.org/10.1017/jfm.2014.78.

[36] H. Teng, H.D. Ng, K. Li, C. Luo, Z. Jiang, Evolution of cellular structures on oblique detonation surfaces, Combust. Flame 162 (2015) 470–477, https://doi.org/10.1016/j.combustflame.2014.07.021.

[37] S.J. Liu, H.Y. P, W.D. Liu, H.L. Zhang, Effects of cavity depth on the ethylene-air continuous rotating detonation, Acta Astronaut. 166 (2020) 1–10, https://doi.org/10.1016/j.actaastro.2019.09.038.

[38] M.P. Burke, M. Chaos, Y. Ju, F.L. Dryer, S.J. Klippenstein, Comprehensive H2/O2 kinetic model for high–pressure combustion, Int. J. Chem. Kinet. 44 (2012) 444–474, https://doi.org/10.1002/kin.20603.

[39] B.J. McBride, M.J. Zehe, S. Gordon, NASA Glenn Coefficients for Calculating Thermodynamic Properties of Individual Species, NASA/TP-2002-211556. NASA Glenn Research Center, Cleveland.

[40] Z. Jiang, On dispersion–controlled principles for non–oscillatory shock–capturing schemes, Acta Mech. Sin. 20 (2004) 1–15, https://doi.org/10.1007/BF02493566.

[41] H.C. Yee, D.V. Kotov, W. Wang, C.W. Shu, Spurious behavior of shock–capturing methods by the fractional step approach: problems containing stiff source terms and discontinuities, J. Comput. Phys. 241 (2013) 266–291, https://doi.org/10.1016/j.jcp.2013.01.028.

[42] N.N. Smirnov, V.B. Betelin, V.F. Nikitin, L.I. Stamov, D.I. Altoukhov, Accumulation of errors in numerical simulations of chemically reacting gas dynamics, Acta Astronaut. 117 (2015) 338–355, https://doi.org/10.1016/j.actaastro.2015.08.013.

[43] N.N. Smirnov, V.B. Betelin, R.M. Shagaliev, V.F. Nikitin, I.M. Belyakov, YuN. Deryuguin, S.V. Aksenov, D.A. Korchazhkin, Hydrogen fuel rocket engines simulation using LOGOS code, Int. J. Hydrogen Energy 39 (2014) 10748–10756, https://doi.org/10.1016/j.ijhydene.2014.04.150.

[44] H. Teng, J. Bian, L. Zhou, Y. Zhang, A Numerical investigation of oblique detonation wave with low Mach numbers in hydrogen–air mixtures, Int. J. Hydrogen Energy 2021 (2021) 10984–10994, https://doi.org/10.1016/j.ijhydene.2020.12.180, 46.

[45] M.A. Liberman, M.F. Ivanov, A.D. Kiverin, M.S. Kuznetsov, Deflagration-to-detonation transition in highly reactive combustible mixtures, Acta Astronaut. 67 (2010) 688–701, https://doi.org/10.1016/j.actaastro.2010.05.024.

[46] N.N. Smirnov, V.F. Nikitin, YuG. Phylippov, Deflagration to detonation transition in gases in tubes with cavities, J. Eng. Phys. Thermophys. 83 (2010) 1287–1316, https://doi.org/10.1007/s10891-010-0448-6.

[47] N.N. Smirnov, V. F Nikitin Sh Alyari-Shourekhdeli, Transitional regimes of wave propagation in metastable systems, Combust. Explo. Shock+ 44 (2008) 517–528, https://doi.org/10.1007/s10573-008-0080-3.

[48] S. Kao, J.E. Shepherd, Numerical solution methods for control volume explosions and ZND detonation structure, in: Tech. Rep. GALCIT Report FM2006.007, California Institute of Technology, Pasadena, California, 2008.

[49] B. Varatharajan, F.A. Williams, Chemical–kinetic descriptions of high–temperature ignition and detonation of acetylene–oxygen–diluent systems, Combust. Flame 124 (2001) 624–645, https://doi.org/10.1016/S0010-2180(00)00235-2.

[50] T. Lu, C.K. Law, A Criterion based on computational singular perturbation for the identification of quasi steady state species: a reduced mechanism for methane oxidation with NO chemistry, Combust. Flame 154 (2008) 761–774, https://doi.org/10.1016/j.combustflame.2008.04.025.